Biochimica et Biophysica Acta 1837 (2014) 1447–1453

Contents lists available at ScienceDirect

Biochimica et Biophysica Acta

journal homepage: www.elsevier.com/locate/bbabio

# Identification of the basic amino acid residues on the PsbP protein involved in the electrostatic interaction with photosystem II ☆

Taishi Nishimura [a], Chihiro Uno [b], Kunio Ido [a], Ryo Nagao [b], Takumi Noguchi [b], Fumihiko Sato [a], Kentaro Ifuku [a,c,*]

[a] Graduate School of Biostudies, Kyoto University, Sakyo-ku, Kyoto 606–8502, Japan
[b] Graduate School of Science, Nagoya University, Aichi 464–8602, Japan
[c] Japan Science and Technology Agency, PRESTO, 4-1-8 Honcho Kawaguchi, Saitama 332–0012, Japan

ARTICLE INFO

*Article history:*
Received 31 October 2013
Received in revised form 28 November 2013
Accepted 25 December 2013
Available online 2 January 2014

*Keywords:*
Extrinsic protein
Higher plants
Oxygen-evolving complex
Photosystem II
PsbP

ABSTRACT

The PsbP protein is an extrinsic subunit of photosystem II (PSII) that is essential for photoautotrophic growth in higher plants. Several crystal structures of PsbP have been reported, but the binding topology of PsbP in PSII has not yet been clarified. In this study, we report that the basic pocket of PsbP, which consists of conserved Arg48, Lys143, and Lys160, is important for the electrostatic interaction with the PSII complex. Our release-reconstitution experiment showed that the binding affinities of PsbP-R48A, -K143A, and -K160A mutated proteins to PSII were lower than that of PsbP-WT, and triple mutations of these residues greatly diminished the binding affinity to PSII. Even when maximum possible binding had occurred, the R48A, K143A, and K160A proteins showed a reduced ability to restore the rate of oxygen evolution at low chloride concentrations. Fourier transform infrared resonance (FTIR) difference spectroscopy results were consistent with the above finding, and suggested that these mutated proteins were not able to induce the normal conformational change around the Mn cluster during $S_1$ to $S_2$ transition. Finally, chemical cross-linking experiments suggested that the interaction between the N-terminus of PsbP with PsbE was inhibited by these mutations. These data suggest that the basic pocket of PsbP is important for proper association and interaction with PSII. This article is part of a Special Issue entitled: Photosynthesis Research for Sustainability: Keys to Produce Clean Energy.



## 1. Introduction

The photosynthetic oxygen-evolving reaction is the basis for the light-to-chemical energy conversion, and is catalyzed by the pigment–protein complex called photosystem II (PSII) [1]. Much progress has been made toward determining the structure of the PSII complex [2–4], and recent X-ray structural analysis of the cyanobacterial PSII complex at atomic resolution has revealed the exact location of subunits, pigments, and cofactors, including the exact organization of the subunits within PSII [5]. The PSII complex is composed of more than 20 proteins, including both membrane-intrinsic and membrane-extrinsic subunits. On the thylakoid luminal side of PSII, a metal cluster consisting of four Mn ions, one $Ca^{2+}$, and five oxo ligands (the Mn cluster) catalyzes the oxygen-evolving reaction. Additionally, two $Cl^-$ ions are bound near the Mn cluster and act as indispensable cofactors for the reaction.

The Mn cluster is surrounded by several membrane-extrinsic subunits within the PSII complex. Together with the loop regions of several membrane-intrinsic subunits such as D1, D2, CP43, and CP47, these support the proper assembly and stabilization of the Mn cluster. This complex is called the oxygen-evolving complex (OEC), and the membrane-extrinsic subunits are referred to as the OEC proteins. Although the composition of membrane-intrinsic PSII core subunits is highly conserved among photo-oxygenic organisms, the composition of the membrane-extrinsic subunits has undergone significant evolutionary change [6]. Green plants such as higher plants, green algae, and euglena have a set of three OEC proteins [PsbO (33 kDa), PsbP (23 kDa), and PsbQ (17 kDa)]. In contrast, cyanobacteria feature PsbV (Cytochrome (Cyt) *c*550) and PsbU (12 kDa) instead of PsbP and PsbQ [7,8]. However, it has been reported that cyanobacteria also possess PsbP and PsbQ homologs, CyanoP and CyanoQ [9,10]. The current view is that PsbV and PsbU were lost during evolution, and PsbP and PsbQ in green plants seem to have evolved from CyanoP and CyanoQ respectively [11]. The crystal structures of isolated PsbP and PsbQ have been ascertained using high-resolution X-ray crystallography [12–15], and locations and binding topologies of PsbP and PsbQ in the green

*Abbreviations:* Chl, chlorophyll; Cyt, cytochrome; DCMU, 3-(3,4-dichlorophenyl)-1,1-dimethylurea; EDC, 1-ethyl-3-(3-dimethylaminopropyl) carbodiimide; FTIR, Fourier transform infrared resonance; MCT, mercuric cadmium telluride; NSP, *N*-succinimidyl propionate; OEC, oxygen-evolving complex; PVDF, polyvinylidene difluoride; PSII, photosystem II; sulfo-NHS, *N*-hydroxysulfosuccinimide; SDS-PAGE, sodium dodecyl sulfate-polyacrylamide gel electrophoresis; WT, wild-type

☆ This article is part of a Special Issue entitled: Photosynthesis Research for Sustainability: Keys to Produce Clean Energy.

* Corresponding author. Tel.: +81 75 753 6381; fax: +81 75 753 6398.
*E-mail address:* ifuku@kais.kyoto-u.ac.jp (K. Ifuku).

0005-2728/$ – see front matter © 2013 Elsevier B.V. All rights reserved.
http://dx.doi.org/10.1016/j.bbabio.2013.12.012

plant PSII complex have been proposed [16,17]. However, these models have not yet been verified, because it has not yet been possible to identify the crystal structure of the green plant PSII complex.

It has been reported that PsbP, but not PsbQ, is essential for normal PSII function [18–21]. Recent analysis with Fourier transform infrared resonance (FTIR) difference spectroscopy has suggested that PsbP binding induces protein conformational changes around the Mn cluster to modulate the binding properties of $Ca^{2+}$ and $Cl^{-}$ in PSII [22]. PsbP-Δ15, in which the N-terminus 15-residues were truncated, did not have the ability to induce this protein conformational change, and did not activate the oxygen-evolving reaction of PSII [22,23]. However, the structure of N-terminus 15-residues of PsbP has not yet been resolved. Recent chemical cross-linking experiments suggest that PsbP interacts directly with the Cyt $b_{559}$ α subunit (the PsbE protein) via its N-terminus, and that this interaction is affected by mutation of His144, which is located in the C-terminal domain [24]. Furthermore, FTIR analysis showed that PsbP-H144A does not induce the conformational change around the Mn cluster during the $S_1/S_2$ transition, nor does it restore oxygen-evolving activity at low chloride concentration. These findings suggest that it is important for PsbP to interact cooperatively with PSII complex via both its N- and C-terminal domains to support oxygen-evolving activity. However, the nature of the interaction between the C-terminal domain of PsbP and the PSII complex is still unclear.

In this study, we investigated the binding topology of the C-terminal domain of PsbP in the PSII complex, using site-directed mutagenesis analysis. Crystal structure of PsbP suggests that it has an asymmetric charge distribution with pronounced positively (basic) and negatively (acidic) charged surfaces (Fig. 1). In particular, there is a positively charged (basic) pocket within the C-terminal anti-parallel β-sheet, which is composed of conserved basic amino acids (Arg48, Lys143, and Lys160) [12]. These basic residues are located near the His144, suggesting that this basic pocket is involved in functional interaction with PSII complex. To investigate the importance of these basic amino acid residues, we created mutated PsbP proteins in which relevant basic amino acids were substituted with Ala, and used release–reconstitution experiments followed by FTIR analysis to examine their functional properties. The results demonstrate that the basic pocket of PsbP consisting of conserved Arg48, Lys143, and Lys160 is important for its interaction with PSII complex. Our data provide crucial information about the binding topology of PsbP in the higher plant PSII complex.

## 2. Materials & methods

### 2.1. Plasmid construction, recombinant protein expression, and purification

The expression plasmids for the mutated PsbP proteins K11A, K13A, R48A, K143A, K160A, R48A/K143A, and R48A/K143A/K160A were constructed using a site-directed mutagenesis kit (Agilent). We used the following primers and associated complementary primers: K11A, 5′-CTGCTAATGTATTCGGGGCGCCAAAGAAAAACACC-3′; K13A, 5′-CTAA TGTATTCGGGAAGCCAGCGAAAAACACCGAATTCATG-3′; R48A, 5′-CCCT GGTCAAGTTTTGGCGTACGAGGACAACTTTG-3′; K143A, 5′-GGTGATGA GGGTGGAGCACACCAAGTAATTG-3′; K160A, 5′-GCTTTACATCTGCGCG GCTCAAGCTGGAG-3′.

The recombinant WT and mutated PsbP proteins were expressed in the *Escherichia coli* strain BL21(DE3) and purified as described by Ifuku and Sato [25]. The presence of the desired mutation in each recombinant PsbP protein was confirmed using MALDI-TOF mass spectrometry (Autoflex III; Bruker Daltonics).

### 2.2. Reconstitution experiments

Spinach oxygen-evolving PSII membranes were prepared using methods previously reported [26]. Spinach leaves used to isolate PSII membranes were purchased at a local market. The chlorophyll (Chl) concentration was calculated using equations described by Arnon [27]. The rate of oxygen-evolving activity in the isolated PSII membranes was ~562 μmol $O_2$ (mg Chl)$^{-1}$ $h^{-1}$. Reconstitution of the recombinant PsbP protein to NaCl-washed PSII membranes was performed following the procedure reported by Ido et al. and Kakiuchi et al. [24,28]. To compare the binding affinities of mutated PsbP proteins with PSII membranes, reconstitution was performed using PsbP:PSII molar ratios of 0.25:1, 0.5:1, 1:1, 2:1, 4:1, 8:1, and 10:1. SDS-PAGE separation was performed using the standard procedure. Gels were stained using Flamingo (Bio-Rad) and visualized using a fluorescent image analyzer (FLA-3000; GE Healthcare). The amount of PsbP bound to PSII was determined by measuring fluorescence intensity using Multi Gauge Ver. 3.0 (GE Healthcare). The rate of oxygen-evolution was measured as described by Ido et al. [24]. To measure oxygen-evolving activity in the presence of various concentrations of $Cl^{-}$, NaCl was added to the buffer used for activity measurement.

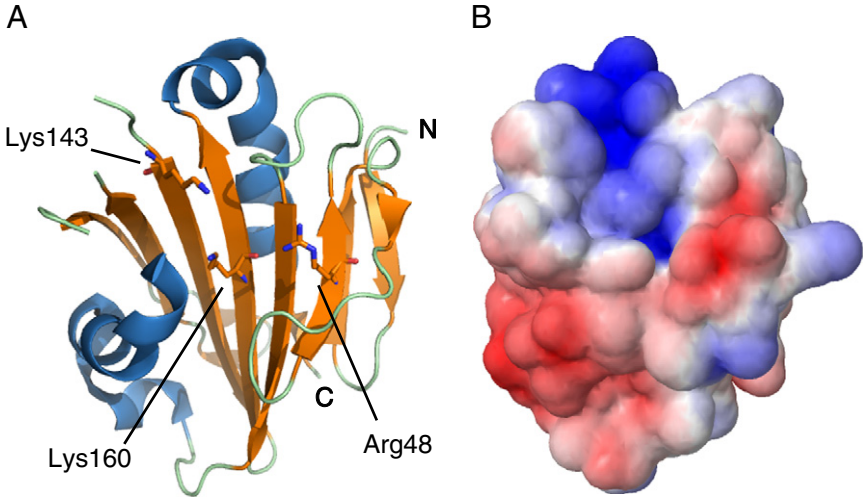


**Fig. 1.** (A) A structural model of spinach PsbP [PDB_ID: 2VU4]. α-helix and β-strands are shown in *blue* and *orange*, respectively. The N (residue 16) and C (residue 186) termini are labelled. The side chains of the Arg48, Lys143, and Lys160 are shown as *stick models*. (B) The electrostatic surface potential of spinach PsbP. Acidic and basic surfaces are color-coded from −5 V (*red*) to 5 V (*blue*).

### 2.3. FTIR analysis

FTIR measurements were performed as reported previously [22,24,28]. PSII samples in the presence of 0.1 mM DCMU were centrifuged, and the resulting pellet was sandwiched between $CaF_2$ plates. Light-induced $S_2Q_A^-$-minus-$S_1Q_A$ difference spectra (hereafter $S_2Q_A^-/S_1Q_A$ spectra) were recorded using an IFS-66/S spectrophotometer (Bruker Optics) equipped with an MCT detector (Infrared D313L, Bruker Optics) at a resolution of 4 $cm^{-1}$ [29]. Illumination was provided by a Q-switched Nd:YAG laser (Spectra-Physics INDI-40-10, 532 nm, ~7 ns full width at half-maximum, ~7 mJ $pulse^{-1}$ $cm^{-2}$ at the sample surface). The sample temperature was adjusted to 250 K in a cryostat (DN1704, Oxford Instrument) using a controller (ITC-5, Oxford Instrument). Single-beam spectra (150 s scan) were recorded before and after single-flash illumination and a difference spectrum was calculated. Samples were warmed to 285 K to relax the $S_2Q_A^-$ charged pair, and then cooled down again to 250 K. Measurements were repeated three to five times for each sample and then averaged.

### 2.4. Cross-linking experiments

Cross-linking was performed as described by Ido et al. [24]. The NaCl-washed PSII membranes, at a concentration of 0.5 mg Chl $ml^{-1}$, were cross-linked with the recombinant PsbP proteins in cross-linking buffer (25 mM Hepes-NaOH, pH 7.2, 25 mM $CaCl_2$) using 6.25 mM EDC and 5 mM *N*-hydroxysulfosuccinimide (sulfo-NHS). The solution was incubated for 2 h in darkness, and the reaction was terminated by adding ammonium acetate to a final concentration of 0.2 M. The solution was centrifuged for 5 min at 20,400 × *g* at 4 °C, and the resulting pellet was subjected to SDS-PAGE. Proteins separated by SDS-PAGE were transferred to polyvinylidene difluoride (PVDF) membranes and analyzed using specific antibodies. We prepared a rabbit antibody against PsbP. Rabbit antibody against PsbE was purchased from Agrisera.

## 3. Results

### 3.1. Structure and electrostatic surface potential of PsbP

The crystal structures of PsbP from *Nicotiana tabacum* (PDB_ID: 1V2B) and from *Spinacia oleracea* (PDB_ID: 2VU4) have been ascertained using X-ray crystallography [12,13]. The two structures are similar, and the structural model of spinach PsbP used in this study is shown in Fig. 1A. The C-terminal domain of PsbP is composed of an anti-parallel β-sheet with an α-helix on either side, while the N-terminal domain has two short β-strands. The structures of the N-terminus 15-residues and the two loop regions have not yet been resolved. Fig. 1B shows the electrostatic surface potential of spinach PsbP, obtained using the PDB2PQR server [30]. PsbP has an asymmetrical charge distribution with pronounced positively and negatively charged surfaces and also features a basic pocket with conserved basic amino acids (Arg48, Lys143, and Lys160). It has been suggested that these basic residues could be important for the interaction with the PSII complex including the extrinsic PsbO [12]. To examine the importance of the basic pocket of PsbP, we produced PsbP mutant proteins (R48A, K143A, and K160A) and characterized them by release-reconstitution experiments.

### 3.2. Substitution of conserved Arg48, Lys143, and Lys160 of spinach PsbP affects binding affinity with the PSII complex

PSII membranes were treated with 1.5 M NaCl to remove native PsbP and PsbQ proteins. Mutated PsbP proteins were reconstituted with NaCl-washed PSII membranes at PsbP:PSII molar ratios from 0.25:1 to 10:1 (Fig. 2). PsbP-reconstituted PSII membranes were washed to remove unbound proteins and subjected to SDS-PAGE analysis. Quantification of the PsbP bands in SDS-PAGE gels showed

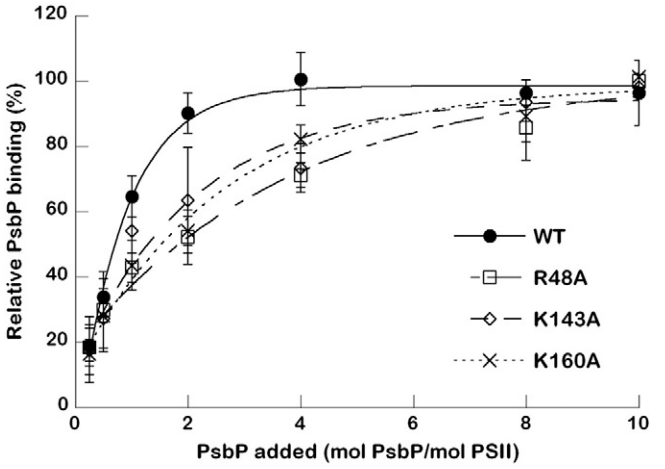


**Fig. 2.** The binding profiles of mutated PsbP proteins to NaCl-washed PSII. NaCl-washed PSII membranes were reconstituted with PsbP-WT (*circles*), PsbP-R48A (*squares*), PsbP-K143A (*diamonds*), and PsbP-K160A (*crosses*) in various molar PsbP:PSII ratios, and the amounts of PSII-bound protein were estimated using SDS-PAGE analysis. A WT:PSII molar ratio of 4:1 was set as 100%; $n = 3$, error bars = S.D.

that maximum binding of PsbP-WT to PSII membranes occurred at a PsbP:PSII molar ratio of approximately 2:1. In contrast, mutated PsbP proteins required a molar ratio of at least 10:1 to fully bind to PSII membranes. This suggests that the binding affinities of these mutated PsbP proteins are weaker than that of the WT protein, and that conserved Arg48, Lys143, and Lys160 are important for association with PSII.

We then measured the oxygen-evolving activity of NaCl-washed PSII membranes reconstituted with mutated PsbP proteins (Fig. 3, *black bars*). Oxygen-evolving activity measurement was performed in the absence of $Ca^{2+}$ and $Cl^-$. PsbPs with double (PsbP-R48A/K143A) and triple (PsbP-R48A/K143A/K160A) mutations and mutations in the N-terminal regions (PsbP-K11A and -K13A) were also prepared and evaluated. Reconstitution of all PsbP species was performed at a 10:1 PsbP:PSII molar ratio. The oxygen-evolving activity of R48A-, K143A-, and K160A-reconstituted PSII membranes was significantly lower than that of WT-reconstituted PSII membranes, although the extent of binding was almost identical to that of the WT protein (Fig. 3, *white*

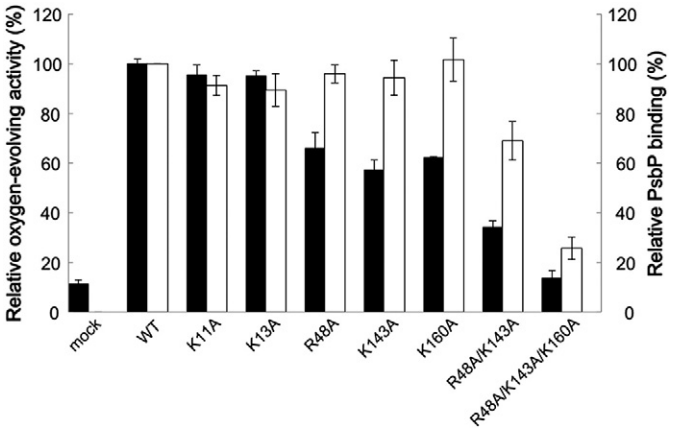


**Fig. 3.** Oxygen-evolving activity and the amount of PSII-bound PsbP in PSII membranes reconstituted with various PsbP mutant proteins. Reconstitution was performed at a molar PsbP:PSII ratio of 10:1. The sample "mock" consisted of NaCl-washed PSII membranes without reconstitution. Oxygen-evolving activity of reconstituted PSII was measured in the absence of $Ca^{2+}$ and $Cl^-$ (*black bars*). The rate of oxygen evolution of WT-reconstituted PSII membranes (442 μmol $O_2$ mg $Chl^{-1}$ $h^{-1}$) was set as 100%; $n = 3$, error bars = S.D. *White bars* indicate the extent of binding of PsbP proteins to PSII membranes. The amount of WT protein bound was set as 100%; $n = 3$, error bars = S.D.

*bars*). This indicates that functional interaction between PsbP and PSII was affected by those mutations. Furthermore, oxygen-evolving activity and the extent of binding were proportionately decreased when the double- and triple-mutated proteins were used. In contrast, the mutation of Lys11 and Lys13, the other conserved basic residues in the N-terminal region, did not affect binding or the rate of oxygen-evolving activity. These results suggest that the basic pocket in the C-terminal domain of PsbP is important for its functional interaction with the PSII complex.

### 3.3. R48A, K143A, and K160A show reduced ability to retain $Cl^-$ in PSII

It has been reported that mutation of His144, located near the basic pocket comprising Arg48, Lys143, and Lys160, leads to a reduced ability in PSII to retain $Cl^-$ [24]. We therefore examined the dependence of the oxygen-evolving activity of WT-, R48A-, K143A-, and K160A-reconstituted PSII membranes on $Cl^-$ concentration (Fig. 4). Mutated PsbP proteins were reconstituted with NaCl-washed PSII membranes at a PsbP:PSII molar ratio of 10:1, and oxygen-evolving activity was measured in the presence of various concentrations of $Cl^-$. The maximum rate of oxygen evolution of WT-reconstituted PSII membranes was achieved at approximately 2 mM $Cl^-$, and greater concentrations of $Cl^-$ gradually decreased this rate. In contrast, the maximum rates of R48A-, K143A-, and K160A-reconstituted PSII membranes were achieved at 10 mM $Cl^-$. These data suggest that while R48A, K143A, and K160A proteins can bind to the PSII complex with a lower affinity, they lose the ability to suppress the $Cl^-$ requirement of oxygen-evolving activity in PSII.

Recent studies using FTIR spectroscopy suggested that reconstitution of PSII membranes with PsbP restores the conformational change around the Mn cluster, and that this conformational recovery is relevant to $Cl^-$ binding in PSII [22,24]. Because the ability to retain $Cl^-$ in PSII is affected by R48A, K143A, and K160A mutations, FTIR spectroscopy was applied to examine whether they are able to restore the conformational change. Fig. 5 shows the $S_2Q_A^-/S_1Q_A$ difference spectra of untreated, NaCl-washed, and PsbP (WT or mutants)-reconstituted PSII membranes. It has already been shown that the effects of extrinsic proteins on the $S_2Q_A^-/S_1Q_A$ spectra are basically identical to those on the $S_2/S_1$ spectra [22,24], and hence the conformational changes around the Mn cluster can be detected by this measurement. When PsbP and PsbQ were removed from PSII membrane by washing with NaCl, the spectra features in the 1700–1600 $cm^{-1}$ region were significantly altered without large changes in other regions (Fig. 5Ab) [22]. Bands in this region arise from the amide I vibrations (C = O stretches of backbone amides) of polypeptide main chain, and hence the spectral changes indicate the dissociation of PsbP and PsbQ triggered the conformational changes around the Mn cluster. These changes in the amide I region are expressed more clearly in an untreated-minus NaCl-washed double difference spectrum (Fig. 5Ba). When PsbP-WT was reconstituted, amide I bands recovered (Figs. 5Ac, 5Bb), whereas reconstitution of K143A and K160A did not recover the bands (Fig. 5Ad, e, and Fig. 5Bc, d) and the spectra were similar to those of NaCl-washed PSII membranes (Figs. 5Ab and 5Ba). The R48A partially recovered the amide I bands, although some changes were still observed (Figs. 5Af and 5Be). These data suggest that binding of R48A-, K143A-, and K160A-mutated PsbP proteins does not properly restore the protein conformations around the Mn cluster, which are required for $Cl^-$ retention in PSII. The smaller effect of R48A mutation may indicate that the manner of interaction of Arg48 is rather different from that of Lys143 and Lys160.

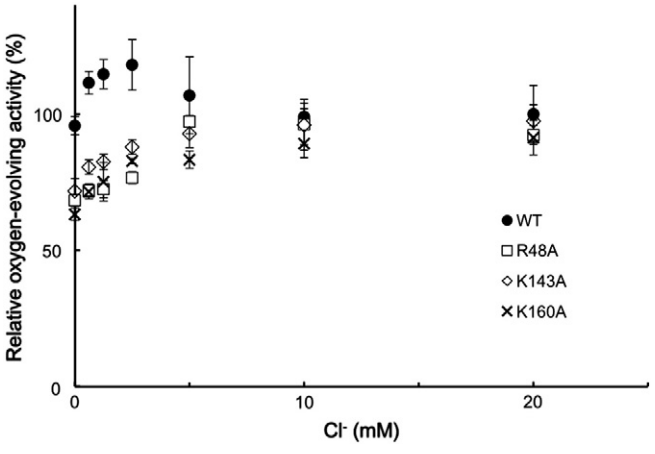


**Fig. 4.** The dependence of oxygen-evolving activity of WT-, R48A-, K143A-, and K160A-reconstituted PSII on $Cl^-$ concentration. The oxygen-evolving activity of WT- (*circles*), R48A- (*squares*), K143A- (*diamonds*), and K160A- (*crosses*) reconstituted PSII was measured in the presence of concentrations of $Cl^-$ from 0–20 mM. The rate of oxygen evolution of WT-reconstituted PSII membranes in the presence of 20 mM $Cl^-$ was set as 100% (339–380 μmol $O_2$ mg $Chl^{-1}$ $h^{-1}$, measured in independent experiments); $n = 3$, error bars = S.D.

### 3.4. R48A, K143A, and K160A mutations affect the interaction between PsbP and PsbE

The exact binding site of PsbP to the green plant PSII complex has not yet been elucidated, although it has been reported that PsbP interacts with PsbE, a cytochrome $b_{559}$ α subunit of the PSII complex [24,31]. PsbP interacts with PsbE via its N-terminus, which is important for ion retention in PSII. To examine whether the Arg48, Lys143, and Lys160 mutations affect the interaction between PsbP and PsbE, chemical cross-linking experiments using EDC and sulfo-NHS were performed (Fig. 6). EDC, a zero length cross-linker, cross-links a primary amine and a carboxyl group that are electrostatically associated. Sulfo-NHS stabilizes the intermediate products of cross-linking and increases EDC cross-linking efficiency. SDS-PAGE analysis followed by immunoblotting showed that the quantities of PsbP-PsbE cross-linked product at approximately 33 kDa were significantly decreased in the R48A-, K143A-, and K160A-reconstituted PSII compared with WT-reconstituted PSII membranes. This confirms that the mutation of conserved Arg48, Lys143, and Lys160 on PsbP impairs the interaction between the N-terminus of PsbP and PsbE.

## 4. Discussion

This study provides crucial information about the binding topology of PsbP protein in the higher plant PSII complex. The mutational analyses showed that PsbP-R48A, -K143A, and -K160A mutant proteins exhibited lower binding affinities with PSII membranes (Fig. 2), and that double and triple mutations of these residues proportionately lowered the binding affinity with PSII (Fig. 3). In addition, the R48A, K143A, and K160A mutant proteins lost the ability to retain $Cl^-$ required for oxygen-evolving activity in PSII (Fig. 4), and FTIR analysis suggested that these mutated proteins did not induce proper conformation around the Mn cluster, which would retain $Cl^-$ in PSII (Fig. 5). Furthermore, cross-linking experiments with zero-length cross-linker EDC showed that interaction between the N-terminus of PsbP and the cytochrome $b_{559}$ α subunit (PsbE) was inhibited in the mutated PsbP proteins (Fig. 6). These data strongly indicate that the basic pocket on PsbP, consisting of conserved Arg48, Lys143, and Lys160, is important for functional interaction with the PSII complex.

Tohri et al. suggested that positively charged lysyl residues in PsbP are important for electrostatic interaction with PSII by chemical modification with *N*-succinimidyl propionate (NSP), which modifies primary amino groups [32]. They surmised that Lys11, Lys13, Lys33, Lys38, Lys143, Lys166, Lys170, and Lys174 of PsbP would be involved in the interaction with PSII. In this report, we suggest that Arg48 and Lys160 of PsbP are also involved in the functional association with the PSII complex. Lys160 would not be modified by NSP, probably since it is located inside the basic pocket in the PsbP structure. We recently

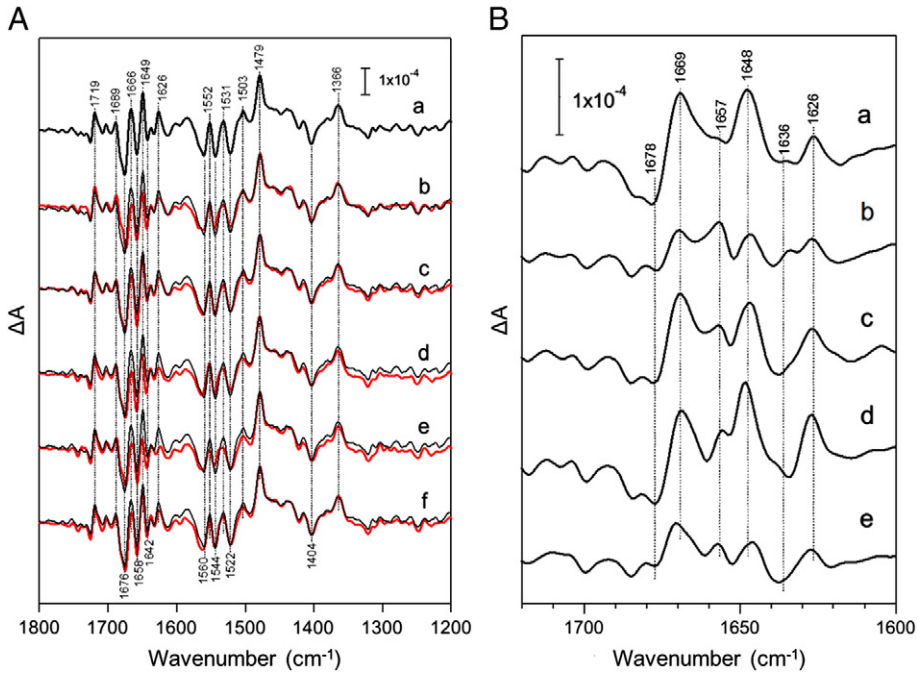


**Fig. 5.** (A) $S_2Q_A^-/S_1Q_A$ FTIR difference spectra of untreated (a, *black line*), NaCl-washed (b, *red line*) and PsbP-reconstituted (c–f, *red lines*) PSII membranes. The spectrum of the untreated PSII membrane is also shown overlapping the spectra of the treated samples (b–f, *black lines*). PSII membranes were reconstituted with WT- (c), K160A- (d), K143A- (e), and R48A- (f) PsbP proteins. (B) Untreated-minus-treated double difference spectra of the $S_2Q_A^-/S_1Q_A$ FTIR spectra in the amide I region. (a) NaCl-washed (PsbP and PsbQ-depleted) PSII. (b–e) PSII reconstituted with WT- (b), K160A- (c), K143A- (d), and R48A- (e) PsbP.

reported that mutation of His144 affects the interaction between the N-terminus of PsbP and PsbE as well as the ability to induce proper conformational change around the Mn cluster to retain $Cl^-$ in PSII [24]. Because similar results were observed in PSII reconstituted with R48A, K143A, and K160A, it is reasonable to consider that the local structures around the conserved basic amino acid residues (Arg48, Lys143, Lys160, and His144) are involved in the association with the PSII complex. It is also likely that they have a role in keeping the N-terminus of PsbP in exactly the right position in PSII to induce proper conformation around the $Cl^-$ binding site. On the other hand, we showed that the mutation of

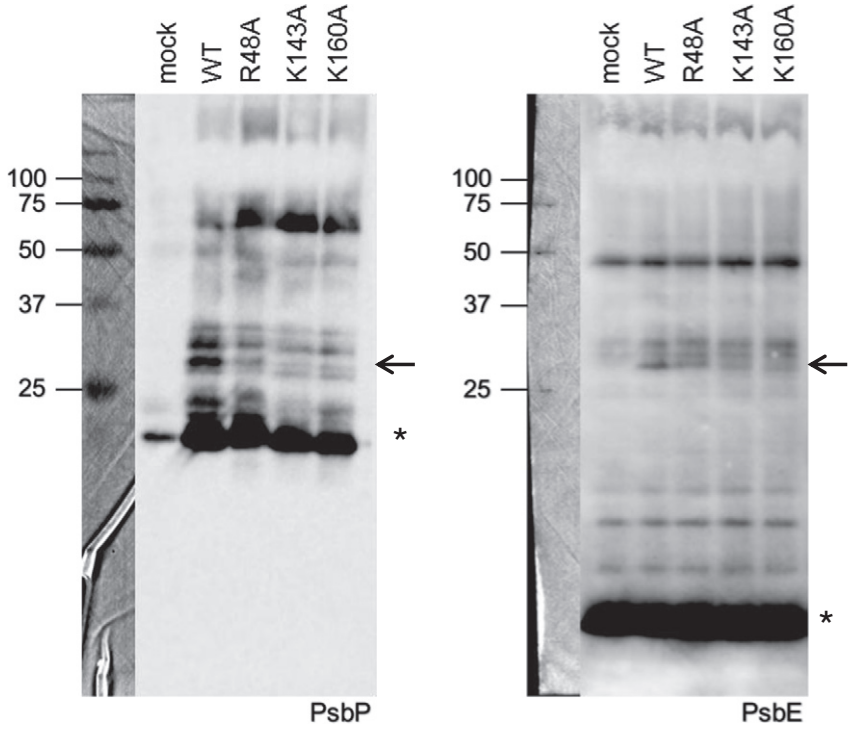


**Fig. 6.** Cross-linking of PsbP mutant proteins with PSII membranes, using EDC and sulfo-NHS. NaCl-washed PSII membranes were cross-linked with WT, R48A, K143A, and K160A. Proteins corresponding to 2 μg Chl were loaded onto each lane and detected with antisera against PsbP or PsbE. Arrows around 33 kDa indicate the cross-linked peptide including PsbP and PsbE. Original positions of PsbP (23 kDa) and PsbE (9 kDa) are indicated by asterisks.

Lys11 and Lys13, conserved in the PsbP's N-terminal domain, did not affect the interaction with the PSII complex (Fig. 3), while previous analysis using N-terminal truncated mutants suggested that Lys11 and Lys13 could be involved in the interaction with the PSII complex [33]. This suggests that Lys11 and Lys13 are dispensable when the overall structure of the N-terminal region is preserved.

We compared the electrostatic surface potentials of PsbP from *Spinacia oleracea* and CyanoP [34], and PsbV [35] from *Thermosynechococcus elongatus*, obtained from the PDB2PQR server (Fig. 7). CyanoP has an almost exclusively negatively charged surface, which is completely different from higher plant PsbP (Fig. 7A, B). Furthermore, the local structure around the basic pocket in the spinach PsbP structure is different from that of CyanoP. In the CyanoP structure, the relevant surface looks like a "cleft" rather than a "pocket", which suggests that it binds to PSII complex with a different, unknown binding partner [36]. A

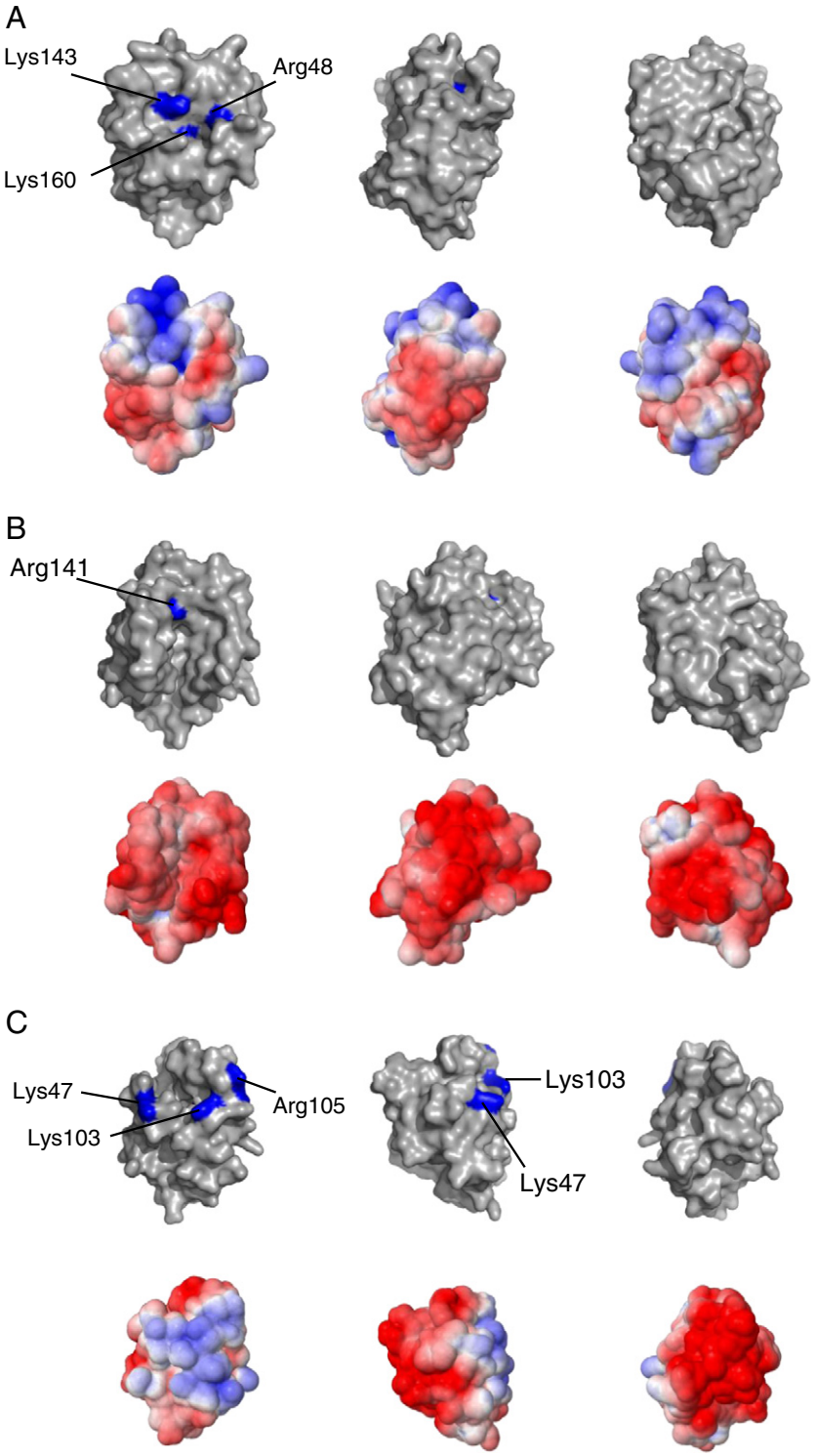


**Fig. 7.** Molecular surfaces and electrostatic potentials of (A) PsbP from *Spinacia oleracea* [13], and (B) CyanoP and (C) PsbV from *Thermosynechococcus elongatus* [34,35]. Electrostatic surface potentials were obtained from the PDB2PQR server [30]. The molecules are rotated anticlockwise by 90° and 180° around a vertical axis (left to right). Acidic and basic surfaces are color-coded from −5 V (*red*) to 5 V (*blue*).

comparison of the amino acid sequences of PsbP homologs shows that Arg48 and Lys160 in PsbP are not conserved, while Lys143 is substituted for Arg in CyanoP [37]. It is suggested that CyanoP possesses a lipid moiety on its N-terminus to anchor itself to the thylakoid membranes [10], and its association with thylakoid membranes is sensitive to detergent treatment [38] but resistant to high-salt or alkaline Tris treatment in *Synechocystis* sp. PCC 6803 [39]. This suggests that the interaction between CyanoP and the PSII complex is not electrostatic, and the mechanism of the interaction of CyanoP with PSII is quite different from that of higher plant PsbP.

In contrast, PsbV has an asymmetric charge distribution on its surface, and interacts with the PSII complex via its positively charged surface in cyanobacterial PSII structure (Fig. 7C). In the *T. vulcanus* PSII complex, PsbV is located on the luminal side of the membrane-intrinsic proteins D1 and CP43, and extends its N-terminus toward PsbE [5]. In the interface with CP43, PsbV has conserved basic amino acid residues (Lys47 and Arg105) that seem to associate with CP43 [40]. In addition, Lys103 in PsbV appears to participate in a charge–pair interaction with Glu83 of CP43, although this lysyl residue is not always conserved in other cyanobacterial species. These facts suggest that the nature of the interaction seems to be conserved between PsbP and PsbV, and that PsbP may take the place of PsbV in cyanobacterial PSII complex. The localization of PsbP in the CP43 side of the PSII monomer is inconsistent with recent proposals locating PsbP on the D2-CP47 side [17,41]. Indeed, we recently detected an interaction between PsbP and CP43 in spinach PSII membranes (K. Ifuku, unpublished results). Further elucidation of the exact binding sites of CyanoP and PsbP in the PSII complex will provide valuable information about the evolutionary relationships among PsbP, CyanoP, and PsbV.

## Acknowledgements

This work was supported in part by a grant from JST PRESTO (Ke.I.) and by a Grant-in-Aid for Young Scientists (B) from JSPS (Grant no. 18770032 to Ke.I.).

## References

[1] G. Renger, T. Renger, Photosystem II: the machinery of photosynthetic water splitting, Photosynth. Res. 98 (2008) 53–80.
[2] K.N. Ferreira, T.M. Iverson, K. Maghlaoui, J. Barber, S. Iwata, Architecture of the photosynthetic oxygen-evolving center, Science 303 (2004) 1831–1838.
[3] B. Loll, J. Kern, W. Saenger, A. Zouni, J. Biesiadka, Towards complete cofactor arrangement in the 3.0 Å resolution structure of photosystem II, Nature 438 (2005) 1040–1044.
[4] A. Guskov, J. Kern, A. Gabdulkhakov, M. Broser, A. Zouni, W. Saenger, Cyanobacterial photosystem II at 2.9-Å resolution and the role of quinones, lipids, channels and chloride, Nat. Struct. Mol. Biol. 16 (2009) 334–342.
[5] Y. Umena, K. Kawakami, J.R. Shen, N. Kamiya, Crystal structure of oxygen-evolving photosystem II at a resolution of 1.9 Å, Nature 473 (2011) 55–60.
[6] T.M. Bricker, J.L. Roose, R.D. Fagerlund, L.K. Frankel, J.J. Eaton-Rye, The extrinsic proteins of Photosystem II, Biochim. Biophys. Acta 1817 (2011) 121–142.
[7] J.R. Shen, Y. Inoue, Binding and functional properties of two new extrinsic components, cytochrome *c*-550 and a 12-kDa protein, in cyanobacterial photosystem II, Biochemistry 32 (1993) 1825–1832.
[8] J.R. Shen, M. Qian, Y. Inoue, R.L. Burnap, Functional characterization of *Synechocystis* sp. PCC 6803 delta *psbU* and delta *psbV* mutants reveals important roles of cytochrome *c*-550 in cyanobacterial oxygen evolution, Biochemistry 37 (1998) 1551–1558.
[9] Y. Kashino, W.M. Lauber, J.A. Carroll, Q. Wang, J. Whitmarsh, K. Satoh, H.B. Pakrasi, Proteomic analysis of a highly active photosystem II preparation from the cyanobacterium *Synechocystis* sp. PCC 6803 reveals the presence of novel polypeptides, Biochemistry 41 (2002) 8004–8012.
[10] L.E. Thornton, H. Ohkawa, J.L. Roose JL, Y. Kashino, N. Keren, H.B. Pakrasi, Homologs of plant PsbP and PsbQ proteins are necessary for regulation of photosystem II activity in cyanobacterium *Synechosistis* 6803, Plant Cell 16 (2004) 2164–2175.
[11] I. Enami, T. Suzuki, O. Tada, Y. Nakada, K. Nakamura, A. Tohri, H. Ohta, I. Inoue, J.R. Shen, Distribution of the extrinsic proteins as a potential marker for the evolution of photosynthetic oxygen-evolving photosystem II, FEBS J. 272 (2005) 5020–5030.
[12] K. Ifuku, T. Nakatsu, H. Kato, F. Sato, Crystal structure of the PsbP protein of photosystem II from *Nicotiana tabacum*, EMBO Rep. (2004) 362–367.
[13] J. Kohoutova, I.K. Smatanova, J. Brynda, M. Lapkouski, J.L. Revuelta, J.B. Arellano, R. Ettrich, Crystallization and preliminary crystallographic characterization of the extrinsic PsbP protein of photosystem II from *Spinacia oleracea*, Acta Crystallogr. Sect. F: Struct. Biol. Cryst. Commun. 65 (2009) 111–115.
[14] V. Calderone, M. Trabucco, A. Vujicić, R. Battistutta, G.M. Giacometti, F. Andreucci, R. Barbato, G. Zanotti, Crystal structure of the PsbQ protein of photosystem II from higher plants, EMBO Rep. 4 (2003) 900–905.
[15] M. Balsera, J.B. Arellano, J.L. Revuelta, J. De Las Rivas, J.A. Hermoso, The 1.49 Å resolution crystal structure of PsbQ from photosystem II of *Spinacia oleracea* reveals a PPII structure in the N-terminal region, J. Mol. Biol. 350 (2005) 1051–1060.
[16] J. Nield, J. Barber, Refinement of the structural model for the Photosystem II supercomplex of higher plants, Biochim. Biophys. Acta 1757 (2006) 353–361.
[17] K. Ifuku, K. Ido, F. Sato, Molecular functions of PsbP and PsbQ proteins in the photosystem II supercomplex, J. Photochem. Photobiol. B 104 (2011) 158–164.
[18] K. Ifuku, Y. Yamamoto, T.A. Ono, S. Ishihara, F. Sato, PsbP protein, but not PsbQ protein, is essential for the regulation and stabilization of photosystem II in higher plants, Plant Physiol. 139 (2005) 1175–1184.
[19] X. Yi, S.R. Hargett, H. Liu, L.K. Frankel, T.M. Bricker, The PsbP protein is required for photosystem II complex assembly/stability and photoautotrophy in *Arabidopsis thaliana*, J. Biol. Chem. 282 (2007) 24833–24841.
[20] Y. Allahverdiyeva, M. Suorsa, F. Rossi, A. Pavesi, M.M. Kater, A. Antonacci, L. Tadini, M. Pribil, A. Schneider, G. Wanner, D. Leister, E.M. Aro, R. Barbato, P. Pesaresi, Arabidopsis plants lacking PsbQ and PsbR subunits of the oxygen-evolving complex show altered PSII super-complex organization and short-term adaptive mechanisms, Plant J. 75 (2013) 671–684.
[21] K. Ido, K. Ifuku, Y. Yamamoto, S. Ishihara, A. Murakami, K. Takabe, C. Miyake, F. Sato, Knockdown of the PsbP protein does not prevent assembly of the dimeric PSII core complex but impairs accumulation of photosystem II supercomplexes in tobacco, Biochim. Biophys. Acta 1787 (2009) 873–881.
[22] M. Tomita, K. Ifuku, F. Sato, T. Noguchi, FTIR evidence that the PsbP extrinsic protein induces protein conformational changes around the oxygen-evolving Mn cluster in photosystem II, Biochemistry 48 (2009) 6318–6325.
[23] K. Ifuku, T. Nakatsu, R. Shimamoto, Y. Yamamoto, S. Ishihara, H. Kato, F. Sato, Structure and function of the PsbP protein of photosystem II from higher plants, Photosynth. Res. 84 (2005) 251–255.
[24] K. Ido, S. Kakiuchi, C. Uno, T. Nishimura, Y. Fukao, T. Noguchi, F. Sato, K. Ifuku, The conserved His-144 in the PsbP protein is important for the interaction between the PsbP N-terminus and the Cyt $b_{559}$ subunit of photosystem II, J. Biol. Chem. 287 (2012) 26377–26387.
[25] K. Ifuku, F. Sato, Importance of the N-terminal sequence of the extrinsic 23 kDa polypeptide in Photosystem II in ion retention in oxygen evolution, Biochim. Biophys. Acta 1546 (2001) 196–204.
[26] D.A. Berthold, G.T. Babcock, C.F. Yocum, A highly resolved oxygen-evolving preparation from spinach thylakoid membranes, FEBS Lett. 134 (1981) 231–234.
[27] D.I. Arnon, Copper enzymes in isolated chloroplasts. Polyphenoloxidase in *Beta Vulgaris*, Plant Physiol. 24 (1949) 1–15.
[28] S. Kakiuchi, C. Uno, K. Ido, T. Nishimura, T. Noguchi, K. Ifuku, F. Sato, The PsbQ protein stabilizes the functional binding of the PsbP protein to photosystem II in higher plants, Biochim. Biophys. Acta 1817 (2012) 1346–1351.
[29] T. Noguchi, T. Ono, Y. Inoue, Direct detection of a carboxylate bridge between Mn and $Ca^{2+}$ in the photosynthetic oxygen-evolving center by means of Fourier transform infrared spectroscopy, Biochim. Biophys. Acta 1228 (1995) 189–200.
[30] T.J. Dolinsky, P. Czodrowski, H. Li, J.E. Nielsen, J.H. Jensen, G. Klebe, N.A. Baker, PDB2PQR: expanding and upgrading automated preparation of biomolecular structures for molecular simulations, Nucleic Acids Res. 35 (2007) 522–525.
[31] R. Nagao, T. Suzuki, A. Okumura, A. Niikura, M. Iwai, N. Dohmae, T. Tomo, J.R. Shen, M. Ikeuchi, I. Enami, Topological analysis of the extrinsic PsbO, PsbP, and PsbQ proteins in a green algal PSII complex by cross-linking with a water-soluble carbodiimide, Plant Cell Physiol. 51 (2010) 718–727.
[32] A. Tohri, N. Dohmae, T. Suzuki, H. Ohta, Y. Inoue, I. Enami, Identification of domains on the extrinsic 23 kDa protein possibly involved in electrostatic interaction with the extrinsic 33 kDa protein in spinach photosystem II, Eur. J. Biochem. 271 (2004) 962–971.
[33] K. Ifuku, S. Ishihara, R. Shimamoto, K. Ido, F. Sato, Structure, function, and evolution of the PsbP protein family in higher plants, Photosynth. Res. 98 (2008) 427–437.
[34] F. Michoux, K. Takasaka, M. Boehm, P.J. Nixon, J.W. Murray, Structure of CyanoP at 2.8 Å: implications for the evolution and function of the PsbP subunit of photosystem II, Biochemistry 49 (2010) 7411–7413.
[35] C.A. Kerfeld, M.R. Sawaya, H. Bottin, K.T. Tran, M. Sugiura, D. Cascio, A. Desbois, T.O. Yeates, D. Kirilovsky, A. Boussac, Structural and EPR characterization of the soluble form of cytochrome *c*-550 and of the *psbV2* gene product from the cyanobacterium *Thermosynechococcus elongatus*, Plant Cell Physiol. 44 (2003) 697–706.
[36] S.A. Jackson, M.G. Hinds, J.J. Eaton-Rye, Solution structure of CyanoP from *Synechocystis* sp. PCC 6803: new insights on the structural basis for functional specialization amongst PsbP family proteins, Biochim. Biophys. Acta 1817 (2012) 1331–1338.
[37] N. Sato, Phylogenomic and structural modeling analyses of the PsbP superfamily reveal multiple small segment additions in the evolution of photosystem II-associated PsbP protein in green plants, Mol. Phylogenet. Evol. 56 (2010) 176–186.
[38] M. Aoi, Y. Kashino, K. Ifuku, Function and association of CyanoP in photosystem II of *Synechocystis* sp. PCC 6803, Res. Chem. Intermed. (2014)(in press).
[39] Y. Ishikawa, W.P. Schroder, C. Funk, Functional analysis of the PsbP-like protein (*sll1418*) in *Synechocystis* sp. PCC 6803, Photosynth. Res. 84 (2005) 257–262.
[40] M. Roncel, D. Kirilovsky, F. Guerrero, A. Serrano, J.M. Ortega, Photosynthetic cytochrome *c*550, Biochim. Biophys. Acta 1817 (2012) 1152–1163.
[41] S. Caffari, R. Kouril, S. Kereïche, E.J. Boekema, R. Croce, Functional architecture of higher plant photosystem II supercomplexes, EMBO J. 28 (2009) 3052–3063.